

Chapter

Application of Fluorescent CQDs for Enhancing the Performance of Solar Cells and WLEDs

Pawan Kumar, Shweta Dua, Balaram Pani and Geeta Bhatt

Abstract

Carbon quantum dots (CQDs) are emerging as promising materials for applications like flexible or transparent solar cell, white light emitting diodes (WLEDs), etc. due to their low cost, eco-friendliness, substantial absorption coefficient, wide absorption spectrum, tuneable optical properties, good charge transfer/separation ability, good quantum yield and large two-photon absorption cross-section. They have been employed in solar cells as active absorbing layers, electron acceptors/donors, electron sinks, electron transporting layers (ETL), hole transporting layers (HTLs), dopants, and interlayer spacing. Consequently, such solar cells have exhibited enhanced performance. In contrast to commercial rare-earth phosphors and traditional semiconductor quantum dots (SQDs) (usually toxic), CQDs exhibit wide range of emission characteristics [full width half maxima (FWHM) > 80 nm]. Interestingly, the emission characteristics of these nanomaterials are tuneable which makes them suitable for WLEDs applications. Red-CQDs are gaining importance as they are required to realize the warm WLEDs. Though a lot of work has been done to modulate the properties of CQDs in order to enhance the performance of solar cells and WLEDs, there are immense possibilities to further exploit the potential of CQDs in these applications.

Keywords: carbon quantum dots (CQDs), solar cell, white light emitting diodes (WLEDs)

1. Introduction

Carbon quantum dots (CQDs) are tiny (2–10 nm) quasi-spherical fluorescent nanoparticles having a core-shell structure. It consists of sp^2 and/or sp^3 carbon domains (core) and oxygen and nitrogen-rich functional groups (shell) [1]. CQDs are synthesised by either bottom-up or top-down approaches; however, the bottom-up approach dominates due to being cost-effective and environmentally friendly.

CQDs were accidentally discovered by Xu et al. in 2004 [2] while segregating single-wall carbon nanotubes from carbon soot using gel electrophoresis. CQDs are very popular for their size, fluorescence, water solubility, biocompatibility, chemical inertness, photo-stability, eco-friendliness, and easy and fast synthesis. They have

been widely used in numerous applications like solar cells, WLEDs, drug delivery, bio-imaging, sensing, data encryption, etc. [1, 3, 4].

In addition, CQDs possess excellent optical properties that can be easily tuned or altered by (i) passivating agents, (ii) functional groups, and (iii) doping/co-doping with heteroatoms [1].

They are a perfect choice for application in PL-based sensing systems because they display photoluminescence (PL) behavior that is excitation wavelength-dependent or -independent, have high quantum yield, and has promising analyte binding capabilities. However, majority of the reports show their excitation wavelength-dependent behavior [1, 4].

CQDs have various functional groups on their surface ($-OH$, $-COOH$, $-NH_2$, etc.) resulting from a variety of chemical treatments. Consequently, CQDs have a strong capacity to connect with both organic and inorganic molecules. Chemi-luminescence and electrochemical luminescence are caused by the remarkable electronic properties of CQDs [1, 3].

Solar cell is an electronic device that converts light energy into electricity through the photovoltaic (PV) effect. Low-weight, flexible and transparent solar cells have gained the interest of researchers in past few years due to their charming commercial applications like pliable chargers, transparent door curtains, vehicle glasses, window shades, etc. Various strategies have been adopted to enhance the performance of these solar cells amongst which employment of semiconductor quantum dots (SQDs) is a very common and effective technique. But SQDs have an adverse effect on environment and health of living beings because it contains carcinogenic materials like Cd, Pb, etc. [5]. Therefore, cost-effective and eco-friendly fluorescent CQDs were thought to be a possible alternative to the SQDs. Interestingly, it was observed that CQDs exhibit large absorption coefficients, broad absorption spectra, [6] and good charge transfer/separation ability, good quantum yield, and a large two-photon absorption cross-section [7]. These characteristics suggest that CQDs have good potential to enhance the performance of optoelectronics devices like solar cells and white light emitting diodes (WLEDs). As a consequence, attention toward CQDs for these applications have boomed in recent years.

WLEDs have become a strong contender as the future solid-state lighting sources owing to their advantages of high luminous efficiency, high luminance, and energy conservation. The characteristic broad emission property makes CQDs widely studied in the field of WLEDs [8]. Firstly, CQD-based WLED was prepared simply by coating yellow CQDs on blue GaN chips but these WLEDs exhibited (1) poor color rendering index (CRI), (2) cold emission [correlated color temperature (CCT) > 5000 K], and (3) excessive blue light which are harmful to human retina. The limitations associated with this WLED were due to the lack of a sufficient red component [9]. Therefore, for warm WLEDs (CCT < 4000 K) efficient red emissive CQDs were extensively researched. Alternately, single-component white emission CQDs (SCWE-CQDs) have gained importance for WLEDs applications because of various advantages such as (1) simple device fabrication procedures, (2) no color fading over time, and (3) no phase separation [10, 11]. In addition, the fluorescence-phosphorescence dual emissive CQDs have been reported which could achieve both SCWE and higher theoretical maximum efficiency in electroluminescent WLEDs simultaneously [11].

Present chapter mainly focuses on applications of CQDs in enhancing the performance of solar cells and WLEDs. In solar cells, CQDs have been used as active absorbing layers, electron-transporting layer (ETL), hole-transporting layer (HTL),

donor/acceptor or dopant. In WLEDs, CQDs have been used as a phosphor material in the presence and absence of composite material to produce white emission.

2. Application of CQDs in solar cells

The CQDs have been employed as energy downshift (EDS) material, sensitizer or co-sensitizer, ETL, hole transport layer, donor/acceptor material and dopant in dye-sensitized solar cells (DSSCs), organic solar cells (OSC), perovskite solar cells (PSCs), and other PV cell configurations. Reports show that the addition of CQDs into the various solar cell components has reduced electron recombination, increased charge density, and boosted electron mobility, improved the performance of the PV cells. Enhancing the power conversion efficiency (PCE) of PV devices is essential in propagating green energy technology. Thus, CQDs offer an affordable, safe, and environmentally friendly method to advance PV performance.

2.1 Energy down shift material

96.3% of total solar radiation reaches the earth's surface whose spectrum lies between 250 and 2500 nm. In order to utilize solar energy to its fullest, it is mandatory for the solar cell to absorb the maximum possible solar spectrum. However, it is strenuous to practically accomplish it like in the case of DSSCs, the sensitizer deteriorates by the UV radiation coming from the sun hence adversely affecting the long-term stability of solar cell especially when Ru-free dyes (indoline dyes D149, etc.) are used [12]. There is an increasing demand for Ru-free dyes for low-cost and environmentally friendly PV systems.

Therefore, various strategies have been adopted to address these concerns and one frequently used technique is the use of EDS materials. EDS material absorbs UV photons and produces low-energy photons. CQDs are among the emerging EDS materials due to their low cost, ease of synthesis, eco-friendliness, and excellent absorbance in the UV region and emission in the visible region. In CQD-based DSSCs, CQDs convert the incident UV radiation into visible light, which is then absorbed by the sensitizer layer. This not only protects the DSSCs from UV rays but also improves the external quantum efficiency (EQE) in the 300–400 nm range [1, 13].

Han et al. prepared highly luminescent CQDs (QY = 84.8%, size = 3.7 nm) from citric acid (carbon source) and ethylenediamine (nitrogen source) in the presence of moderate ammonia water (AW) to attain proper inner structure and excellent N-passivation. They used hydrothermal method for synthesis of CQDs. The CQDs were then mixed with polyvinyl alcohol (PVA) aqueous solution (5 wt%) to obtain the CQDs/PVA composite solution. This solution was spin-coated on the silicon nanowire (SiNW) solar cells and heated (80°C for 20 min). This resultant layer serves as the EDS layer. This leads to the enhancement of the PCE from 10.85% to 10.96% which was attributed to the competing result of the deterioration of the surface reflectance and the optical absorption redistribution [14].

Riaz et al. synthesized N-doped CQDs (QY = 70%, size = 5 nm) from citric acid and 2,3-diaminonaphthalene (DAN) by a one-pot hydrothermal method and applied them as EDS in DSSC. EDS layer converted the incident UV radiation (from sun) into green light which was also absorbed by the active layer of DSSC in addition to the already absorbed spectrum. Since more photon absorption took place hence more carriers were generated and improved short circuit current density (J_{SC}) was recorded. EQE

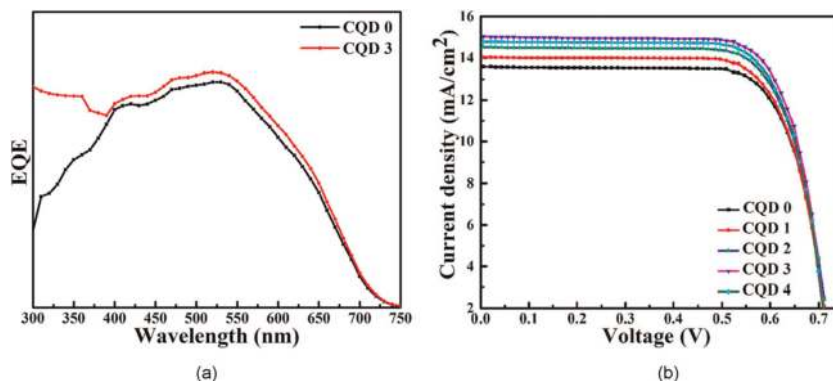


Figure 1.

(a) Enhancement of External quantum efficiency (EQE) in the UV region by the incorporation of CQDs, (b) I-V curve of DSSC at different numbers of coatings (CQD X; X is the number of N-CQDs solution coatings).

test confirmed the enhanced absorption of photons as shown in **Figure 1a**. On the whole, the PCE of the DSSC was amplified in the presence of CQDs as shown in **Figure 1b** and the highest recorded PCE was 8.2% for CQD-3 in comparison to 7.3% for CQD-0. It was observed that the PCEs of CQD-3 and CQD-0 were 6.3% and 2.1%, respectively after 3 weeks which denotes that CQDs layer significantly resists the photo-degradation of sensitizers. Result claims that CQD based EDS layer not only improved the efficiency but also enhanced the stability of the solar cell [15].

Ali et al. synthesised red emissive hollow nitrogen-doped CQDs (NR-CQDs) (QY = 61%, size = 11 nm) from 1, 3-dihydroxy benzene (DHB) and hydrazine monohydrate in the presence of ethanol and NH₄OH by hydrothermal method. They coated NR-CQDs as an EDS layer on crystalline silicon solar cells (c-Si SC). This layer of NR-CQDs absorbed the UV radiation from sun and emitted the red light which was absorbed by the cell in addition to the already coming spectrum and caused the PCE to increase by 5.8% [16].

Lu et al. synthesised CQDs from o-phenylenediamine (oPD) and acetic acid by hydrothermal method. They introduced a luminescent and anti-reflective (AR) silica layer on the top glass of a solar panel (with and without CQDs) for solar panel encapsulation. They found that the improved short-circuit current (I_{SC}) increased the PCE of solar panels from 20.76% (AR coating only) to 20.94% (AR-CQD coating). The improved I_{SC} was attributed to the higher EQE by the AR-CQD coating in the UV range (300–400 nm) in contrast to only AR-coated layer. On contrary, the role of the CQDs was almost insignificant in the remaining spectrum and EQE was slightly lower at longer wavelengths for AR-CQD film. This may be due to the surface scattering caused by the aggregated CQDs in porous silica. The inclusion of CQDs was compatible with the standard AR process of PV glass with no additional cost and it provided a better means for solar panel encapsulation along with enhanced performance [17].

2.2 Sensitizer or co-sensitizer

Sensitizers are photosensitive materials that absorb incoming light and convey the excited electrons to the nearby molecules. Various inorganic and organic/metal-free dyes/natural dyes like N3, N719, N749 (black dye), K19, CYC-B11, C101, K8, D102, SQ, Y123, Z907, etc. have been used as sensitizers in DSSCs.

Among the various dyes available, Ru-based sensitizers (dyes) are commonly used in the most advanced DSSCs. This is because these dyes have carboxylate ligands that anchor the dyes to TiO₂, thus offering excellent stability when adsorbed on TiO₂ surfaces [6, 12]. Although Ru-based sensitizers generally offer excellent performance and have the ability to provide highly efficient DSSCs, their synthesis relies on the rare and expensive Ru metal center, usually, time-consuming and the range of Ru dyes is limited to DSSCs [12, 18]. Thus, Ru-based sensitizers are unfit for economical and environmentally safe PV systems and researchers looked for an alternative. They found that metal-free organic dyes are economical, environmentally safe and have higher absorption coefficient (one order of magnitude higher than Ru complexes) and these dyes started developing at a fast pace.

However, the efficiency based on these dyes is lower than that based on Ru dyes, also these dyes are less stable at high temperatures [18].

As a result, researchers are constantly looking for sensitizers or co-sensitizers that are more appropriate and efficient for solar cells. Due to low cost, sustainability and environmental friendliness, many researchers have tried CQDs as sensitizers or co-sensitizers as new materials and they found superb results [19].

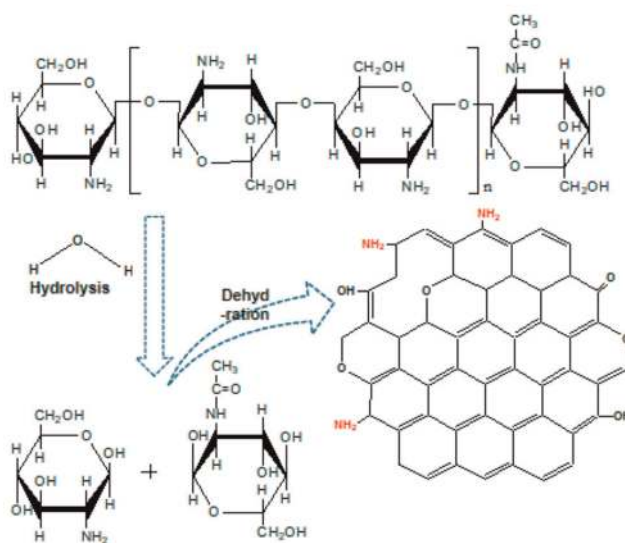
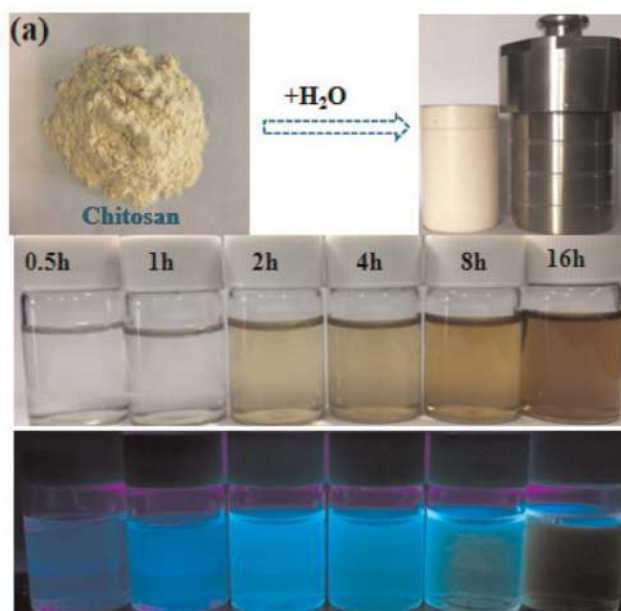
Mirtchev et al. synthesized CQDs (QY = 0.5%, height = 9 ± 6 nm) from g-butyrolactone by chemical ablation (sp² hybridized core with hydroxyl, carboxyl, and sulfonate groups) and used them as sensitizer on the photo-anode of nanocrystalline TiO₂ solar cells. The surface functional groups of CQDs enabled the coordination of CQDs to TiO₂ in a similar manner as done by the carboxylate ligands of the dye. Consequently, the PCE of DSSC was enhanced to 0.13% in comparison to 0.03% (non-sensitized nano-crystalline TiO₂). The enhancement is attributed to the broad absorption spectrum throughout the visible region. However, the J_{SC} reported in their study was much lower than the value routinely obtained through Ru sensitizer-based solar cells. The proposed reason for lower J_{SC} was the presence of various emission trap sites on the CQDs surface that serve as the recombination centers [6].

Wang et al. synthesized the NR-CQDs (QY = 36%, size = 10.8 nm) from citric acid and ammonia for different mass ratios through pyrolysis method. The absorption reaches to maximum value for the mass ratio of 1:4 (ammonia: citric acid). These CQDs were incorporated as sensitizer in the TiO₂-based solar cells and recorded the highest PCE of 0.79% under 1 sun illumination (AM 1.5) at that time. This improved performance of solar cell was due to the rich absorption of CQD/TiO₂ in the visible region and the increased transfer of electron from CQD to the TiO₂ conduction band (CB) [20].

Mistry et al. synthesised un-doped CQDs (QY = 5.2%) and NR-CQDs (QY = 9.8%) and incorporated them as green sensitizers in the TiO₂-based quantum dot (QD) solar cells. CQDs divulged a narrow particle size of 9.5 ± 1.9 nm. The highest recorded PCE was 0.56% (for 0.25% NR-CQDs) which was almost double that of the un-doped CQDs solar cell (PCE = 0.30%) under 1 sun illumination. Under a low light intensity of 0.1 sun illumination (AM 1.5), the PCE of nitrogen-doped (0.25% doping) CQDs-based solar cell was further increased to 1.2%. The presence of nitrogen in CQDs facilitated the injection of photo-carriers into the TiO₂ layer, improving the photo-current and hence the PCE of the solar cell device [21].

Yang et al. synthesized N-CQDs (size = 2 nm) using natural chitosan powders from hydrothermal method for different periods (0.5, 1, 2, 4, 8, 16 hours), as shown in **Figure 2a**. Each of these N-CQDs (having different properties) (**Figure 2b**) was used independently as a co-sensitizer for the DSSC (N719 dye) and consequently

performance of all the cells get enhanced. The highest recorded cell PCE was up to 9.15% (with N-CQDs synthesized for 2 hours) which was much higher than 8.5% for controlled devices (excluding N-CQDs) under 1 standard sun (AM 1.5). This improvement was due to the following reasons: (i) Since, the energy level of N-CQD is in good agreement with the energy level of TiO_2 and the reduction potential of I^-/I_3^- , electrons can be injected into TiO_2 but not into the electrolyte thereby acting as an electron blocking layer (a layer which inhibits the recombination of injected electrons with red-ox pair in the electrolyte). (ii) Under photoexcitation, N-CQD functions as a charge transfer antenna that receives and transfers energy to the N719 dye via Förster or Fluorescence Resonance Energy Transfer Mechanism (FRET). As a result, this mechanism has significantly improved the light absorption capacity of the device. (iii) The optimized N-CQD showed excellent up-conversion emission which broadened the absorbance of the device and improved the capacity to collect long wavelengths [22].



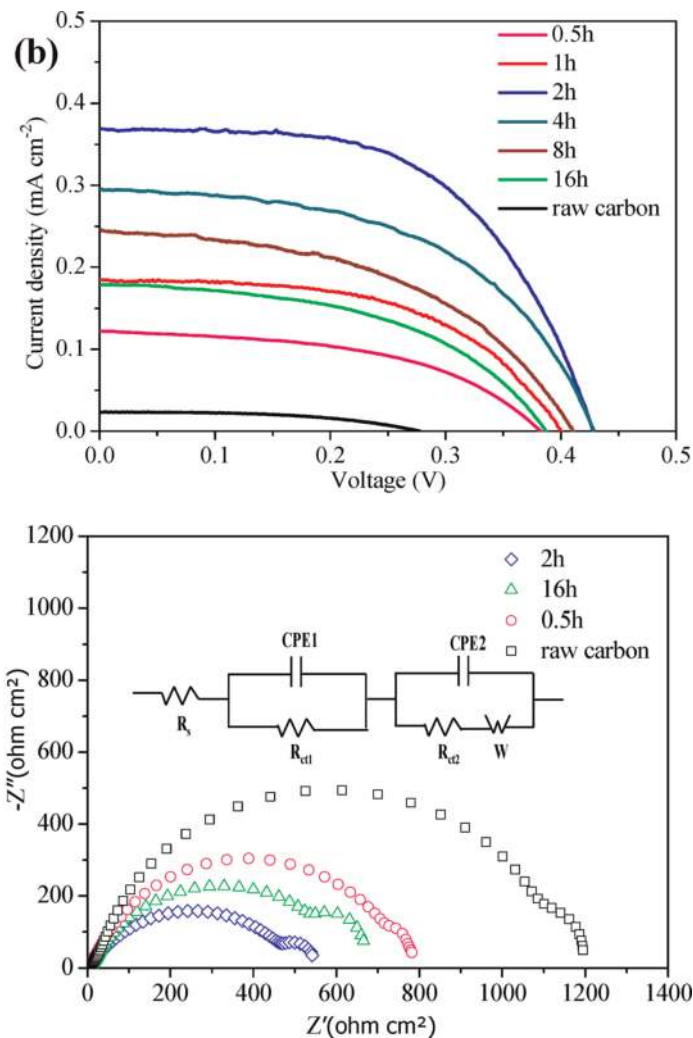


Figure 2. (a) Conversion from chitosan powders to CQDs by a hydrothermal method and images of nitrogen-doped CQDs aqueous solutions for different periods (0.5, 1, 2, 4, 8, 16 hours) under ambient and UV exposure. Each of these N-CQDs possess different properties and (b) Photocurrent density–voltage (J – V) curves for N-CQDs sensitized solar cells under simulated sunlight ($AM1.5$, 100 mW cm^{-2}) and impedance different of solar cells.

2.3 Electron transport layer

The purpose of the ETL (between the active layer and the cathode) is to extract electrons from the active layer towards the cathode and prevent recombination of free electrons and holes at defects present at the interface (active layer to cathode).

Presence of the ETL improves the number of electron transfer from active layer to cathode. TiO_2 and ZnO films are metal oxide ETLs widely used in PSCs, of which TiO_2 is the most reported ETL not only in PSCs but also in DSSCs.

TiO_2 has a HOMO/LUMO position ($-7.63\text{ eV}/-4.4\text{ eV}$) suitable for the extraction and injection of charge carriers, easy to fabricate, and economical. But low electron mobility, high trap-state density below the CB, and relatively high processing temperatures are serious problems.

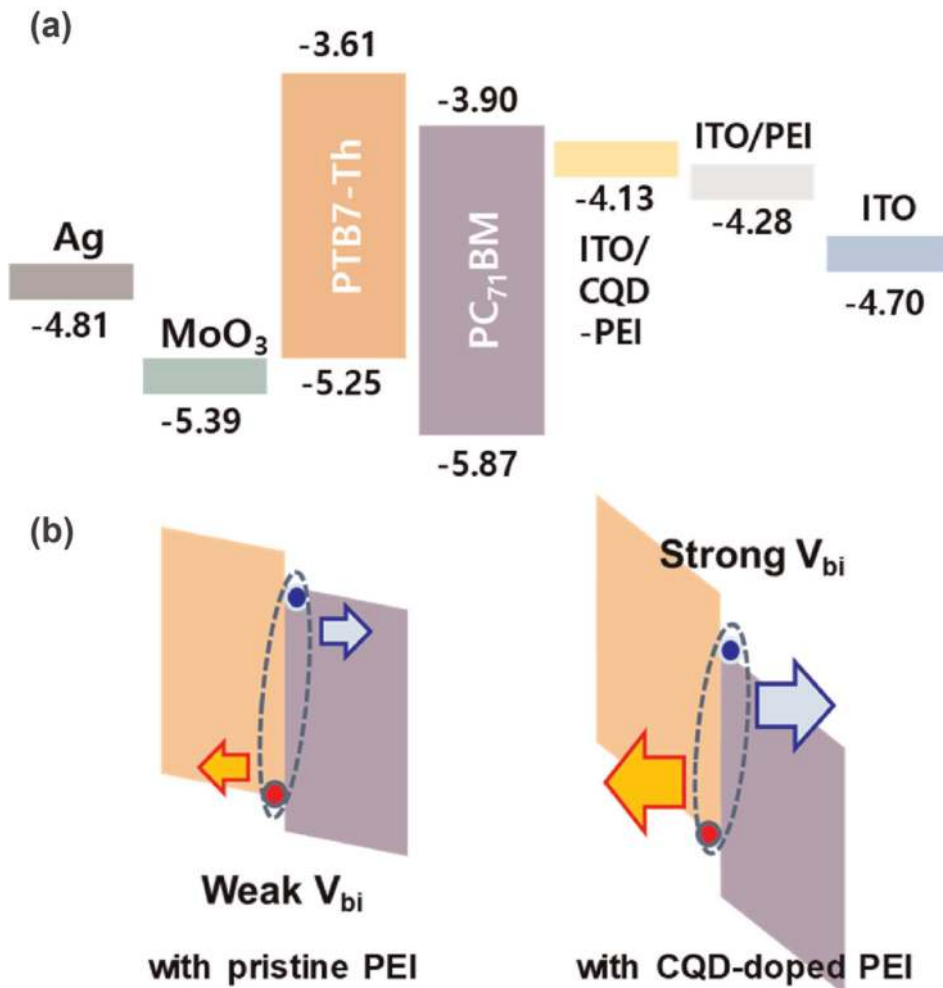
On contrary, ZnO has much higher conductivity than TiO_2 and thus exhibits low recombination loss and does not demand high-temperature therapy.

But like TiO₂, ZnO too has a degradation issue, which turns down the stability of device [18, 23]. It seems, that another ETL material, namely tin oxide (SnO₂), may replace both ZnO and TiO₂ in certain aspects. SnO₂ does not require high-temperature processing, possesses high electron mobility, reasonable HOMO/LUMO position, excellent stability, and high transparency in the visible and near-infrared regions.

Although metal oxide ETLs (TiO₂, ZnO, and SnO₂) are chemically and physically more stable than organic ETLs, they nonetheless contain a disproportionately high number of surface defects and traps when compared to organic ETLs [23].

Among organic ETLs, CQDs have been studied and found to be an emerging contestant in a variety of organic ETL materials. This is due to its excellent photo-stability, low toxicity, excellent electron extraction ability, easy bandgap tuning, etc. CQD as an ETL is deployed by researchers in two ways: (i) replacing existing ETL entirely, or (ii) blending with existing ETL [1].

Yan et al. synthesized the CQDs (size = 3.5 nm) by chemical vapor deposition (CVD) in an Ar atmosphere using C₂H₂ (carbon source). Their group used synthesised CQD as an ETL in fabrication of solution-treated OSCs. According to the results, the optimized PCE of P3HT:PC61BM, PTB7:PC61BM, and PTB7-TH:PC71BM devices (consisting of CQDs as ETLs) reached 3.11%, 6.85% and 8.23%, respectively. These results are comparable with the Lithium fluoride (LiF, one of the ETL) based devices. Due to lower resistance of CQDs-ETL, the interfacial connection between the Al electrode and the active layer was improved. This lower interfacial resistance and



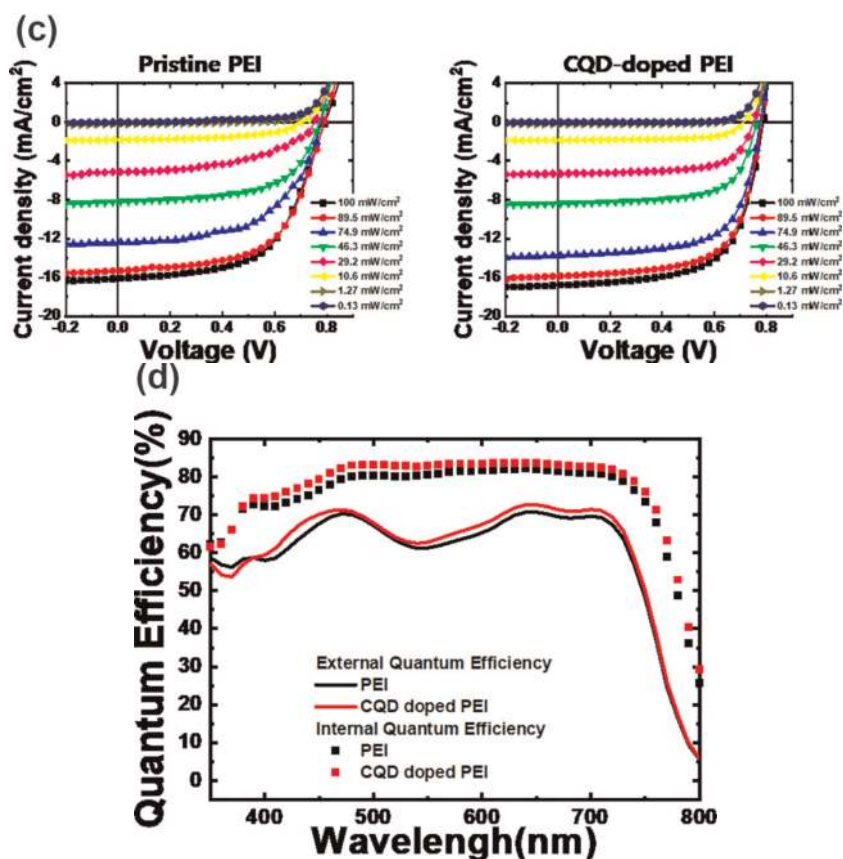


Figure 3. (a) Energy level diagram of PTB7-Th: PC71BM solar cells, (b) CQD-doped PEI induced a stronger internal field due to the lower work-function. This strengthened internal field induced better exciton dissociation efficiency, (c) Current density-voltage characteristics of Pristine CQDs and CQD doped PEI, (d) Quantum Efficiency of Pristine CQDs and CQD doped PEI.

better electron injection resulted in superior device performance. The long-term thermal stability of CQDs-ETLs based devices was also enhanced significantly due to minimised diffusion of CQDs in the active layer [24].

Li et al. synthesized CQDs from glucose via one-step alkali-assisted ultrasonic chemical method. They observed that the PCE of planar n-i-p hetero-junction PSCs were boosted to 18.89% upon incorporation of CQDs/TiO₂ composite layer as ETL.

CQDs improved the electronic coupling between the CH₃NH₃PbI_{3-x}Cl_x and TiO₂ ETL interface, which enhanced the electron transport property (charge extraction and injection) at TiO₂/perovskite (from perovskite to TiO₂). Consequently, enhanced short-circuit current density (J_{SC}), open circuit voltages (V_{OC}), and hence PCE was achieved [25].

Zhu et al. synthesised CQDs (size = 4 nm) via microwave-assisted hydrothermal. They built a planar heterojunction (PHJ) CH₃NH₃PbI₃ PSC using CQDs-doped PCBM as ETL. Doping with CQDs resulted in a PCE of 18.1% (39.2% increase), compared to a PCE of 13% for pure PCBM-based devices. Moreover, CQD doping improved the long-term stability of PSCs by increasing the diffusion of I⁻ [26].

Park et al. synthesized CQDs (size = 3.6 ± 1.2) from neutral red powder and ethylene-diamine via microwave irradiation. These CQDs have NH₂ ligands, these CQDs were incorporated in different ratios in the polyethyleneimine (PEI) layer of fabricated solar cells. In solar cell, the PEI layer modifies (reduce) the work function of ITO, and CQDs in PEI extend this effect as shown in **Figure 3a** and **b**.

Consequently, all the solar cells performed better after incorporation of CQDs (different concentrations).

The impact of CQD concentration on J_{SC} and % EQE are shown in **Figure 3c** and **d**. The highest recorded PCE was $\sim 9.5\%$ (for 2% CQDs) in comparison to PCE of $\sim 8.6\%$ pristine (for 0% CQDs) PEI layer-based solar cells. The enhancement of the performance of CQD-based solar cell was attributed to (i) better electron transport and (ii) improved exciton dissociation probability due to the strengthened internal field [27].

2.4 Hole transport layer

The objective of an HTL (between the anode and active layer) is to extract holes from the active layer towards the anode and to minimize the recombination of free electrons and holes at defects states that exist on the interface (anode and active layer). Presence of the HTL improves the number of holes transferred from active layer to anode. PEDOT:PSS is one of the most widely used HTLs but its strong acidity and hygroscopicity reduce the device stability. In addition, its insulating nature reduces the electrical conductivity (low hole mobility) reduces the device performance, and high cost limits its application [18]. This forced the researchers to explore low-cost and stable material. This brought inorganic p-type materials based HTMs such as CuI, NiO, Cu₂O, CuO, MoO_x, VO_x, WO_x, etc. into PSCs [28]. These inorganic materials exhibit a wider band gap, high conductivity and also prevent the device from exposure to the ambient atmosphere. So, employing such inorganic materials in PSCs could help to achieve higher PCE, yet their sensitivity towards oxygen and moisture seems to be a hindrance. To overcome such sensitivity towards ambient condition, low-cost carbon-based materials like CQDs have been employed as HTLs in solar cells and better performance have been reported. Therefore, in comparison to the aforementioned materials, CQDs emerge as one of the better alternatives [18, 29].

Paulo et al. synthesized CQDs from citric acid and p-phenylenediamine via hydrothermal approach. The cyclic voltammetry (C-V) measurements revealed that the prepared CQD's HOMO and LUMO energy levels are suitable for hole transfer (or electron blocking) from perovskite to CQDs. They incorporated CQDs as the HTL for the very first time in methylammonium lead iodide (MAPI) solar cells and observed a PCE of 3%. This efficiency was quite poor in comparison to another similar device's PCE of 8.06%, which was observed utilizing spiro-oMeTAD as the HTL. According to ESEM analysis of the devices, the poor perovskite coverage across the mp-TiO₂ surface was the cause of the poor performance of CQD-HTL-based device [30].

Nguyen et al. synthesized the N-CQDs (size = 3.32 nm) using fumaronitrile by solvothermal process and O-CQDs (oxidised) using carbon nanofiber via chemical oxidation method. Their idea was to utilize the strength of both PEDOT: PSS and CQDs, consequently they studied the impact of both varieties of CQDs (as HTL) in the presence of PEDOT:PSS on the performance of fabricated solar cells.

They recorded the highest PCE of 8.57% (with N-CQDs), 8.17% (with O-CQDs) and 7.26% (No CQDs) as shown in **Figure 4**. The performance of device was improved because the incorporation of CQDs in PEDOT:PSS drastically (i) decreased the resistance, (ii) raised the work function, (iii) altered the surface energy, and (iv) smoothed the surface morphology of PEDOT:PSS. In addition, it decreased the electrostatic interaction between PEDOT and PSS, which resulted in the π - π

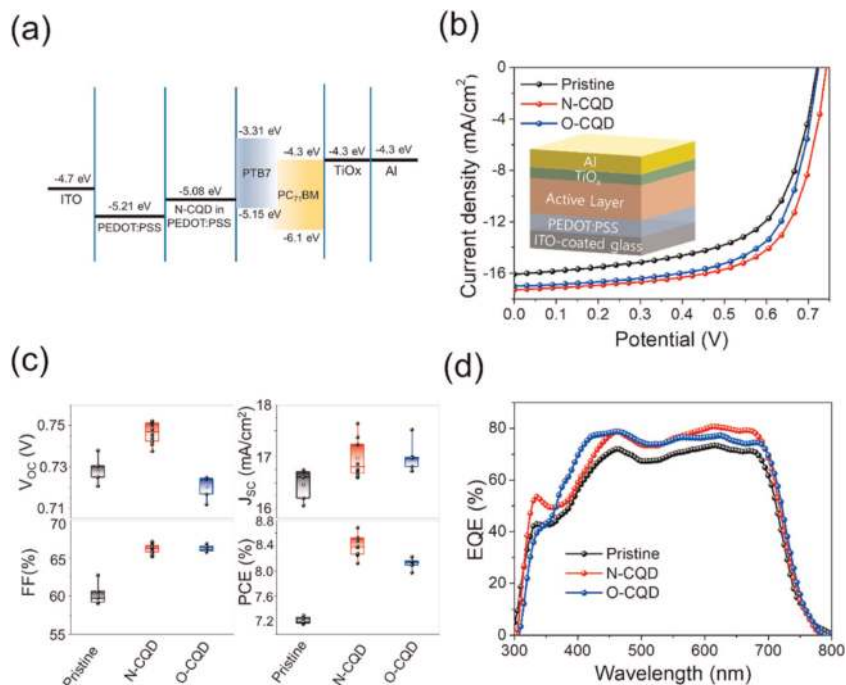


Figure 4. OPV device performance and characterization. (a) Energy band diagram (b) Current density voltage ($J-V$) curves (inset: OPV device with the structure ITO/PEDOT:PSS/active layer/TiOx/Al). (c) Photovoltaic response, and (d) EQE spectra of OPV devices.

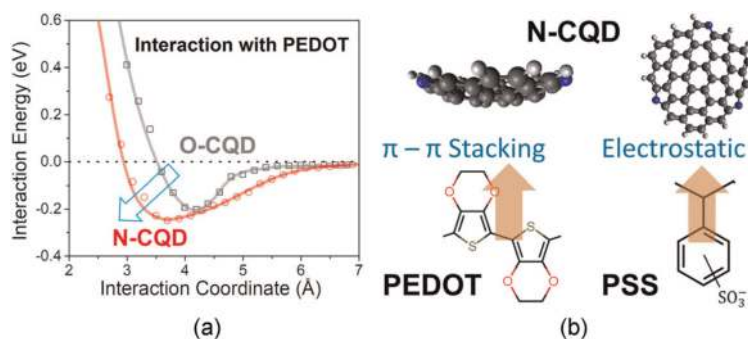


Figure 5. (a) Potential energy scan for each pair of N-CQD/PEDOT and O-CQD/PEDOT; (b) $\pi-\pi$ stacking of PEDOT with N-CQDs and electrostatic interactions of PSS with N-CQDs.

stacking of PEDOT and the hydrophilic interaction of PSS with N-CQDs as shown in **Figure 5**. The interactions in the presence of N-CQDs were quite strong in contrast to O-CQDs. The combination of PEDOT:PSS and N-CQDs improved the charge extraction and charge injection, consequently boosting the improved performance of the solar cells [31].

2.5 Donor/acceptor

In numerous reports, fullerene derivatives have been fully supplanted by CQDs as donor or acceptor material in PV devices [29]. Some research groups have considered the “CQDs as acceptors” when CQDs are incorporated into the active layers. But in

this chapter, we have categorised it separately where CQDs will be considered as “dopant” (CQDs as dopant may either accept or donate electrons).

Feng et al. synthesized CQDs (QY = 12.1%, size = 6.2 nm) from L-ascorbic acid (carbon source) and ethanediamine (catalyst) by a hydrothermal method. They found that integration of as prepared CQDs in P3HT (mass ratio 1:1) drastically quenched the PL of P3HT. Since the energy level of the CQDs was well aligned with those of the P3HT consequently, majority of photo-excited electrons are transferred from P3HT to CQDs instead of undergoing radiative recombination. Hence, quenched PL is observed in the presence of the CQDs [32].

Cui et al. synthesized C-CQDs (size = 3.5 nm) by CVD in an Ar atmosphere using C_2H_2 as a carbon source. They fabricated the inverted OSCs with P3HT as donor and C-CQDs as an acceptor (for different amount of C-CQDs: 0, 2.5, 5.0, and 10 wt% ratio to P3HT) and compared the performances of all the solar cells.

PL quenching was seen in the P3HT:C-CQDs composite film, indicating that photo-induced charge transfer between P3HT and C-CQDs had taken place. V_{OC} and FF were found to increase with the C-CQDs concentration and reached the maximum value for 10 wt% C-CQDs. Similarly, J_{SC} rose with C-CQDs concentration but peaked at 5 wt% C-CQDs before falling.

Consequently, the highest PCE of 0.29% was recorded for 5 wt% C-CQDs based solar cells which were almost 2.5 times higher than device without C-CQD (0.08%) [33].

The enhanced performance of C-CQDs-based solar cell is attributed to the improved absorption by C-CQD:P3HT composite film and effective charge transfer from P3HT (donor) to C-CQDs (acceptor), as shown in **Figure 6**.

They also studied the impact of the hydrothermally produced CQDs (H-CQDs) on the performance of solar cell and found that the PCE was just 0.1% for 5 wt% H-CQDs. The aggregation (poor dispersion) of H-CQDs in the P3HT matrix, [33] which was observed using the FETEM, was the cause of the lower performance with H-CQDs.

Privitera et al. synthesized N-CQDs (size = 2.4 nm) from chlorohydrated arginine and ethylenediamine via assisted hydrothermal methods and functionalized them with various thiophene-containing groups. The purpose of CQD's functionalization was to (i) improve their electron-donating capability and (ii) enhance their solubility in non-polar solvents. They showed that the PL of a thin film of a CQD:PCBM mixture dramatically quenched as a result of the transfer of electrons from the CQDs (donor) to the PCBM (acceptor) which was confirmed electron paramagnetic resonance (EPR). They also noted that various functionalization derivatives on CQDs changed the charge transfer efficiency of the CQD: PCBM blend using time-resolved EPR spectroscopy [34]. There

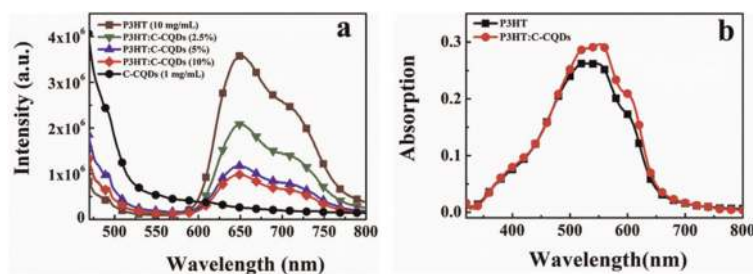


Figure 6. (a) PL spectra of P₃HT (10 mg ml⁻¹), C-CQDs (1 mg ml⁻¹) and P₃HT:C-CQDs (P₃HT: 10 mg ml⁻¹, C-CQDs content: 0, 2.5, 5, and 10 wt% vs. P₃HT) composite films at an excitation of 450 nm. (b) Absorption spectra of P₃HT and P₃HT:C-CQDs (1: 5%) in the solid state.

are currently very few studies that concentrate on CQDs as electron donors, leaving plenty of possibility for additional research to fully realise its potential.

2.6 Dopants

Doping is one of the popular methods used to modify the optoelectronic properties of the base material. According to the reports, CQDs may soon be viable alternative eco-friendly dopant materials for commercial solar cells.

Cui et al. synthesized CQDs (size = 3.5 nm) by CVD in an Ar atmosphere using C_2H_2 as a carbon source. Their group fabricated the several OSCs with P3HT (donor), $PC_{61}BM$ (acceptor) and CQDs (dopant with different concentrations 0, 0.025, 0.05, 0.075 and 0.1 wt%). They noticed when CQDs (dopant) climbed from 0 to 0.075 wt %, the PCE efficiency increased from 3.3% to 3.67% (11% enhancement) while the PCE reduced to 3.55% with a further increase in doping concentration to 0.1 wt%.

The improved PCE of CQDs based solar cell was attributed to (i) the absorption and scattering by well-dispersed CQDs in the active layer, which might improve J_{SC} , and (ii) reduced series resistance of the device that improved J_{SC} and the fill factor (FF) [33].

Shejale et al. synthesised CQDs (size = 2–6 nm) from citric acid and urea by microwave-assisted pyrolysis method. Their group fabricated DSSCs and discovered that after doping the active layer with manufactured N-CQDs (co-active layer) under 1 solar irradiation, the cell's PCE increased to 8.75%. The incorporation of the N-CQDs in the photoactive layer had (i) a synergistic effect on the absorbance and (ii) reduced the recombination between the photo-anode and electrolyte. Their group also employed the N-CQDs as sensitizers and co-sensitizers in DSSCs and consequently, enhanced performance was observed in both situations. However, the highest improvement was recorded when N-CQDs were doped in the active layer (co-active layer). This improvement was attributed to (i) many dye anchoring sites, (ii) strongly conducting photo-anode, (iii) rapid charge carrier transfer, and (iv) intrinsic light-emitting photo-fluorescent characteristics of N-CQDs in mesoporous titania [35].

Table 1 below provides a comparative study of the impacts of CQDs on the performances of various solar cell types.

3. Application of CQDs in WLEDs

WLEDs exhibit interesting characteristics like (1) wider emission spectrum (400–760 nm) (2) high luminous efficiency, (3) high luminance, and (4) energy conservation which make WLEDs a strong candidate for future solid-state lighting sources [8, 37].

There are mainly three methods to realize the WLEDs as shown in **Figure 7**: (1) First, WLED is obtained by encapsulating tricolor chips emitting red, green, and blue (RGB) light. These RGB lights combine to generate white light. However, as service time increases, these tricolor chips show distinct aging properties that can result in different brightness decay and optical stabilities, which restricts the use of such WLEDs. (2) Second, WLEDs are realized by combining a blue LED chip (which emits blue light) and yellow phosphor (which emits yellow light upon excitation by a blue LED chip). The mixture of blue and yellow light produces white emission from one chip. But these WLEDs exhibit (i) low CRI because of less red component, and (ii) the blue LED chip and the yellow phosphor show

Synthesis technique	Type of solar cell [#]	Roll of CQDs	Solar cell structure (with CQD)	A % PCE (without CQD)	B % PCE (with CQD)	% ΔPCE (B-A)	Ref.
Dehydration [chemical oxidation]	NCTiSC	Sensitizer	FTO/TiO ₂ /CQD/electrolyte/Pt-FTO	0.03%	0.13%	0.10%	[6]
Hydrothermal	SiNwSC	EDS layer	Si/SiNWs/CQDs/PVA	10.85%	10.96%	0.11%	[14]
CVD	OSC	ETL	ITO/PEDOT:PSS/active layer/ETL (CQDs)/Al (Active layer = P3HT:PC61BM)	1.75%	3.11%	1.36%	[24]
			ITO/PEDOT:PSS/active layer/ETL (CQDs)/Al (Active layer = PTB7:PC61BM)	6.28%	6.85%	0.57%	
			ITO/PEDOT:PSS/active layer/ETL (CQDs)/Al (Active layer = PTB7-TH:PC71BM)	7.59%	8.23%	0.64%	
Hydrothermal	PSC	HTM	FTO/d-TiO ₂ /mp-TiO ₂ /MAPI/HTM/Au	0.71%	3.00%	2.29%	
Pyrolysis	QDSC	Sensitizer	FTO/TiO ₂ /N-CQD/gel electrolyte/Pt-FTO	—	0.79%	NA	[20]
Alkali-assisted ultrasonic chemical method	PSC	ETL	ITO/CQDs/TiO ₂ /perovskite/spiro-OMeTAD/Au	15.15%	18.89%	3.75%	[25]
CVD	OSC	Electron acceptor	ITO/ZnO/P3HT:C-CQDs/MoO ₃ /Al	0.08%	0.29%	0.21%	[33]
CVD	OSC	Dopant	ITO/ZnO/P3HT:C-CQDs:PC61BM/MoO ₃ /Al	3.30%	3.67%	0.37%	[33]
Hydrothermal	DSSC	EDS layer	FTO/TiO ₂ /CQDs/electrolyte/Pt-FTO	7.30%	8.20%	0.90%	[15]
Microwave irradiation	i-PSC	ETL	FTO/PEDOT:PSS/MAPbI ₃ /PCBM:CQDs/BCP/Ag	16.01%	18.10%	2.09%	[26]
Solvothermal	NCTiSC	Sensitizer	FTO/TiO ₂ /mp-TiO ₂ /CQD/electrolyte/Pt-FTO	—	0.56%	NA	[19]
Hydrothermal	DSSC	Co-sensitizer	FTO/TiO ₂ /N719 dye/CQDs/electrolyte/Pt-Ni-FTO	8.50%	9.15%	0.65%	[22]
Hydrothermal	c-SiSC	EDS layer	Not mentioned	17.39%	18.40%	5.80%	[16]
Microwave irradiation	i-OSC	ETL	ITO/PEI-CQDs/PTB7-Th:PC71BM/MoO ₃ /Ag	8.55%	9.47%	0.92%	[27]
Solvothermal	OSC	HTL	ITO/PEDOT:PSS-CQDs/PTB7:PC71BM/TiO _x /Al	7.26%	8.57%	1.31%	[31]
Pyrolysis	S-TFSC	Absorber layer	ITO/CdS/CCTS:CQD/Al	0.30%	7.00%	6.70%	[36]

Measured %PCE is Under one standard sun (AM 1.5).

[#] NCTiSC: nanocrystalline TiO₂ solar cell, SiNwSC: silicon nanowire solar cells, QDSC: quantum dot solar cell, OSC: Organic solar cell, PSC: perovskite solar cell, DSSC: Dye sensitized Solar cell, i-PSC: inverted perovskite solar cell, c-SiSC: crystalline silicon solar cell, i-OSC: inverted organic solar cell, S-TFSC: Superstrate Thin Film Solar Cell.

Table 1.
Effect of CQDs on the performance of solar cells.

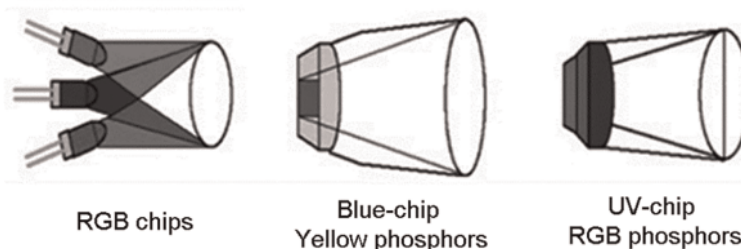


Figure 7.
Diagrammatic representation for three methods to realize the WLEDs.

different changing trends in luminous efficiency over time, resulting in the color change of the WLED.

(3) Third, WLED is obtained by combining near-ultraviolet LED chip (emits UV light) and a fluorescent material (which can effectively produce fluorescence under excitation of near ultraviolet light). This fluorescent material consists of the combination of red/green/blue phosphors (RGB tricolor fluorescent material) or/and the single white-light fluorescent material which upon excitation by UV light generates the white light. Warm WLEDs have been successfully reported using this method [38].

WLED phosphor materials generally include rare earth phosphors, SQDs, and CQDs. Since their research and preparation techniques are rather well-established, rare earth fluorescent elements are frequently employed in WLEDs. However, their extensive application is constrained by the high cost of their raw ingredients and the difficulty in controlling their emission spectrum. Traditional SQDs have poisonous components (Cd, Pb, Hg, etc.), which significantly restricts their practical use. On the other hand; CQDs are inexpensive, environmentally friendly, and easily synthesizable which makes CQDs a promising alternative fluorescent material for WLED application [1, 8, 38]. In addition, CQDs exhibit wide emission characteristics [Vis-NIR, full width half maxima (FWHM) > 80 nm] in contrast to commercial rare-earth phosphors and traditional SQDs.

It results from the robust electron-phonon interaction of the CQD and the greatly dispersed particle size which makes CQDs a perfect material for WLEDs [8, 38].

CQDs are used in three ways for WLEDs: (1) Combination of different CQDs, (2) CQDs with different phosphors, and (3) single CQDs. In WLEDs based on (1) and (2) methods CQDs or/and phosphor materials are excited which consequently generates the white light. However, in both these methods, it is difficult to tune the mixture ratio of multiple phosphors during fabrication device and the distinct light stability of phosphors causes the color shifting of the WLED. On the other hand, WLEDs based on single CQDs consist of CQDs which generate white light by adjusting RGB spectral composition during the phosphor synthesis. This, single SCWE-CQDs based WLEDs have attracted much attention owing to their advantages such as high color quality white emission, easy preparation, no color fading with time, and long lifetime [8, 10, 11, 38, 39].

In order to further imitate the sunlight to achieve high color quality white emission researchers are trying to broaden the emission spectra of CQDs to achieve SCWE emission. As a result, in the realm of current research on fluorescent material for WLEDs, WLEDs based on a single CQD phosphor are emerging.

On the basis of the source of excitation (optical or electrical) WLEDs are divided into two categories which are discussed below:

3.1 Phosphor-converted WLEDs

One of the methods uses CQDs as light-converting phosphors that produce white light when optically pumped by blue or UV LED chips, which are utilised as primary light sources. Sometimes this kind of WLED is referred to as phosphor-converted WLEDs (pc-WLEDs). CQDs-based WLEDs were first prepared simply by coating yellow CQDs on blue GaN chips. These WLEDs exhibited CCT > 5000 K (cold WLEDs), inferior CRI, and excessive blue light which was due to the lack of a sufficient red component. The strong blue light from these chips is harmful to human retina and therefore, warm WLEDs (CCT < 4000 K) containing enough red emission are becoming increasingly important [8, 9].

Wang et al. have developed R-CQDs (QY up to 53%) as the red phosphors and using this in combination with our blue emissive CQD (B-CQD) and green emissive CQD (G-CQD) phosphors, we have realized a UV-pumped CQD phosphor-based warm WLED with the commission internationale de l'elclairage (CIE) coordinates, CCT and CRI of (0.3924, 0.3912), 3875 K and 97 (**Figure 8**). The luminous efficiency of the optimized warm WLED was as high as 31.3 lm W^{-1} , which is similar to that of SQD and rare earth phosphor-based WLEDs [40].

Zhu et al. fabricated WLEDs by combining white-emitting CQDs dispersed in epoxy resin and a UV-chip (370 nm), with the CIE coordinate (0.277, 0.362) which approached the coordinate (0.33, 0.33) of pure white light [41].

Meng et al. coated solid ultra-BWCQDs on the surface of the UV-LED chip (400 nm) to produce warm WLEDs. The WLEDs exhibited full width at half maximum over 200 nm throughout the entire visible light window, with a sufficient red component with CIE coordinates of (0.42, 0.38) and a high CRI value of 91 [10]. In comparison to the commercial WLED lamp (CRI \approx 85), the warm WLED lamp is more capable of showing the true colors of the fruits. **Figure 9** shows (a) photograph of the warm WLED lamp, (b) EL spectrum of the solid ultra-BWCQDs, (c) Fruit colors under the commercial warm WLED lamp, and (d) fruit color under the solid ultra-BWCQD warm WLED lamp.

The CCT and CRI values showed a very slight change with increase of drive current from 20 to 120 mA. These results show that the warm white light generated from the warm WLED lamp has a high color chromatic stability against an increase in drive current [10].

Recently, Li. et.al. prepared environmentally friendly white fluorescent carbon dots (CDs)/ZnO QDs and employed them for making WLEDs. Prepared WLED exhibited fluorescence emission spectra ranging from 425 nm to 750 nm, CIE chromaticity coordinate of (0.30, 0.34) (as shown in **Figure 10**), and a color temperature of 7093 K [42].

3.2 Electroluminescent WLEDs

Yuan et al. synthesised multicolor bandgap fluorescent carbon quantum dots (MCBF-CQDs) from blue to red with quantum yield up to 75% by solvothermal method.

Using MCBF-CQDs as an active emission layer, their group fabricated monochrome electroluminescent LEDs (mc-ELLEDS) for the first time. The maximum

luminance of blue LEDs reaches 136 cd m^{-2} , which is the best performance for CQD-based mc-ELLEDs. MCBF-CQDs-based energy level diagram of mc-ELLEDs, emission spectrum of MCBF CQDs and mc-ELLEDs are shown in **Figure 11a** and **b**.

Their group also fabricated WLED using green bandgap fluorescent-CQDs (G-BF-CQD) blended *N*-vinyl carbazole (PVK) as an emissive layer. Prepared WLED showed a broad EL emission spectrum with two emission peaks centered at about

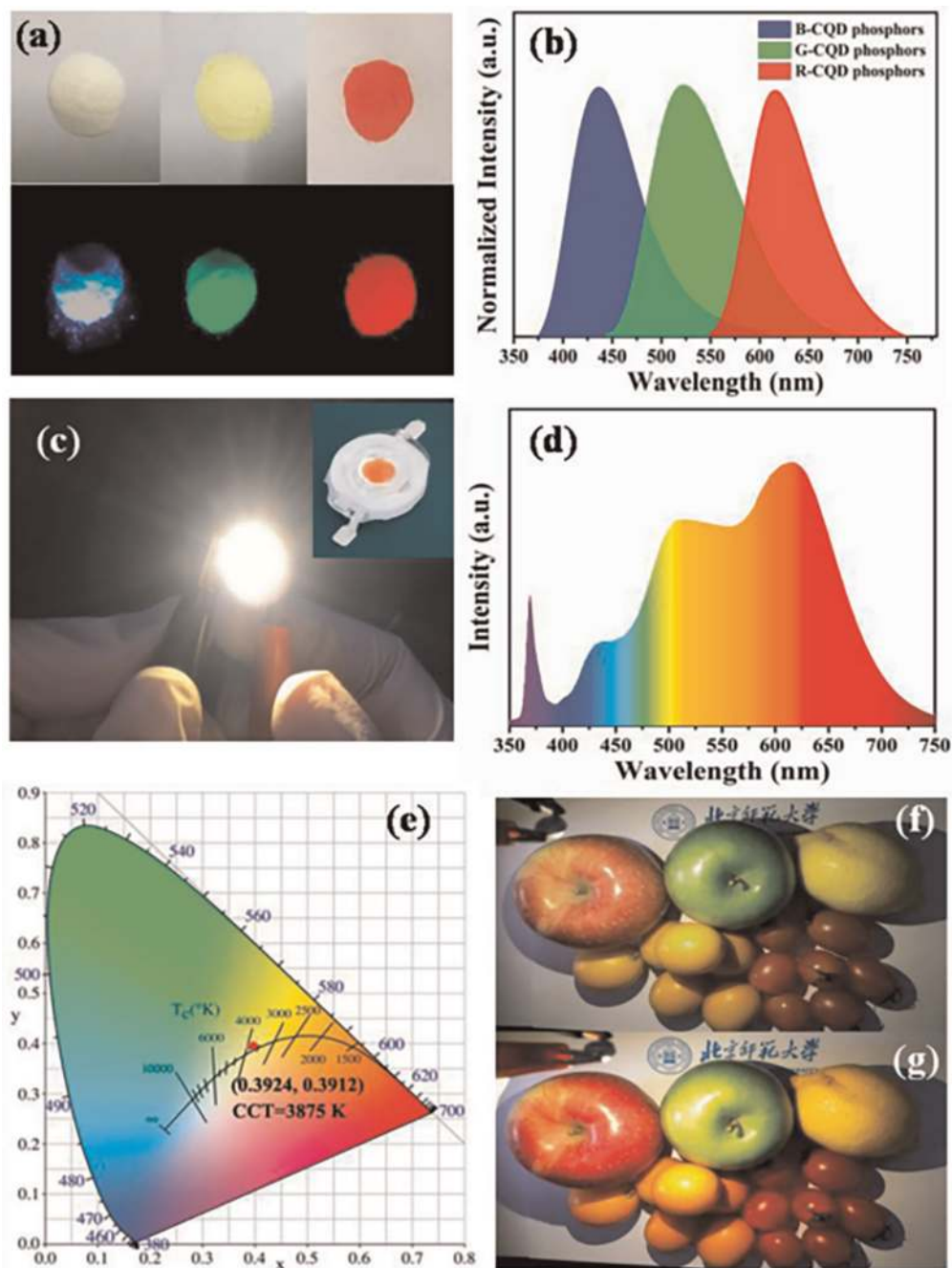


Figure 8. (a) Image of Blue, Green and Red Phosphor CQDs under sunlight (above) and UV light (below), (b) their corresponding spectrum emission, (c) Photograph of warm WLED lamp (inset) and the operating warm WLED lamp (d) Electro luminance Spectrum, (e) CIE color coordinate of the warm WLED lamp. Fruit color under (f) commercial WLED lamp and (g) CQD warm WLED lamp.

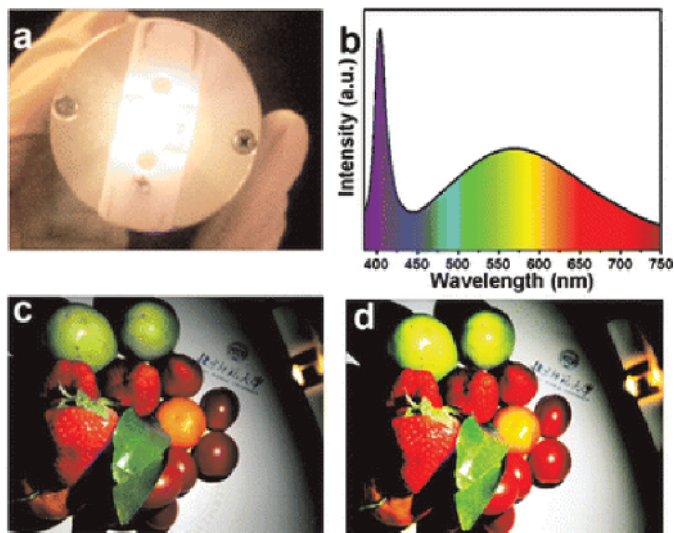


Figure 9. (a) Photograph of the warm WLED lamp, (b) EL spectrum of the solid ultra-BWCQDs, (c) Fruit colors under the commercial warm WLED lamp, and (d) fruit color under the solid ultra-BWCQD warm WLED lamp.

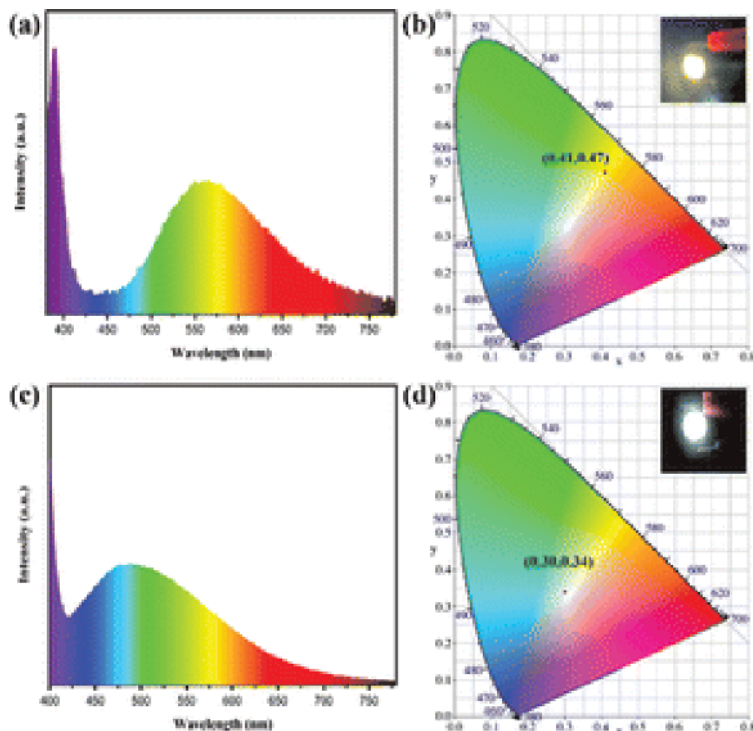


Figure 10. CIE chromaticity coordinate.

410 and 517 nm (**Figure 11c**), which are associated with the emission of PVK and G-BF-CQDs respectively with CIE coordinates at (0.30, 0.33) as shown in **Figure 11d**. The maximum luminance (L_{\max}) and η_c reached about 2050 cd m^{-2} and 1.1 cd A^{-1} respectively with low turn ON voltage (V_{on}) of about 3.9 V which is comparable to QDs-LEDs [43].

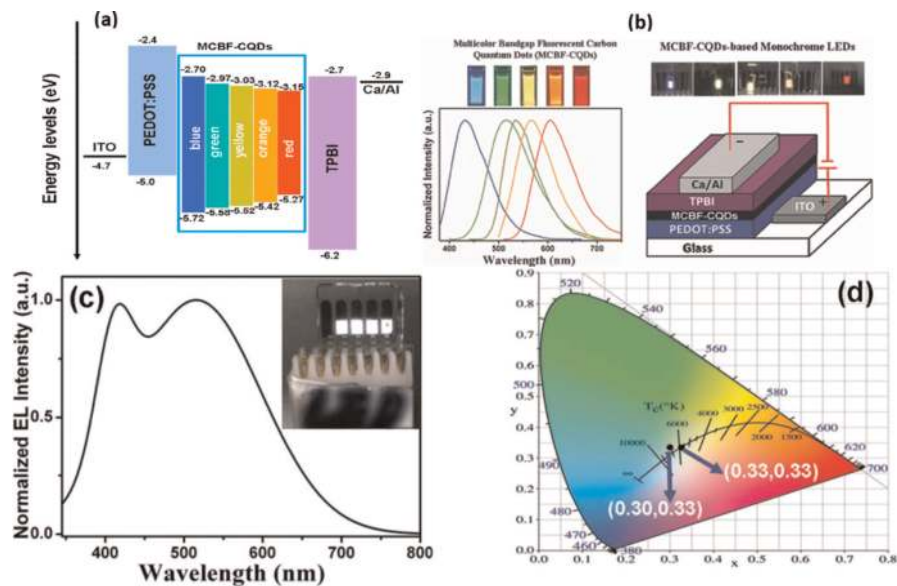


Figure 11. (a) MCBF-CQDs-based energy level diagram of monochrome electroluminescent LEDs, (b) Emission spectrum of MCBF-CQDs from blue to red along with the monochrome electroluminescent LEDs, (c) broad EL emission spectrum with two emission peaks centered at about 410 and 517 nm, (d) two emission peaks which are associated with the emission of PVK and G-BF-CQDs respectively with CIE coordinates at (0.30, 0.33).

However, owing to the lack of red component, these cold WLEDs are not the best choice for indoor lighting. Combined with the blue emission stemming from PVK and the broad red emission from the R-CQDs-NMe₂, -NEt₂, and -NPr₂, the corresponding CIE coordinate and CCT warm WLEDs-1, -2, and -3 are (0.379, 0.314)/3365 K, (0.383, 0.311)/3168 K, and (0.388, 0.309)/2987 K (WLEDs-3), respectively [44]. Taking advantage of the high QYs which were up to 86% in ethanol, the L_{\max} and $\eta_{c\max}$ of the LEDs reach as high as about 5248–5909 cd m⁻², 3.65–3.85 cd A⁻¹. It was the first time to realize high-performance CQDs based electroluminescent warm-WLEDs which was attributed to the CQD's high-efficiency bandgap red emission and good solubility. Additionally, portions of the SCWE-CQDs were utilised as the active emission layers in the electroluminescent WLEDs [45]. However, the efficiency of these types of WLEDs was decreased due to the surface defect-state emission nature, the weaker luminescence, and the poorer carrier transfer performance.

Luo et al. synthesized white emission graphene quantum dots (GQDs) using graphite (precursor) via microwave-assisted hydrothermal method, and thus fabricated a solution-processed WLED, which shows CIE (0.24, 0.25) at the applied voltage of 14 V (**Figure 12a**) near to that of pure white light (0.33, 0.33). The EQE of this WLED was 0.24%, 0.21%, 0.20%, and 0.19% for 11, 12, 13, and 14 V applied voltages, respectively (**Figure 12b**) [46].

Paulo-Mirasol et al. reported white CDs based WLEDs at voltage close to 5 V with a CIE of (0.284, 0.291) as well, while the L_{\max} is only 21 cd A⁻¹ [45].

Recently, Rao et al. obtained extremely photoluminescent SCWE-CQDs by carefully regulating the dilution ratios between the pure red carbon quantum dots (RCQDs) solution and *N,N*-dimethylformamide (DMF) with relative PLQY around 53%.

They were able to produce white light with CIE (0.328, 0.336), which is close to pure white light (0.33, 0.33), and corresponding CRI and CCT values of 84 and 5710 K, respectively [47].

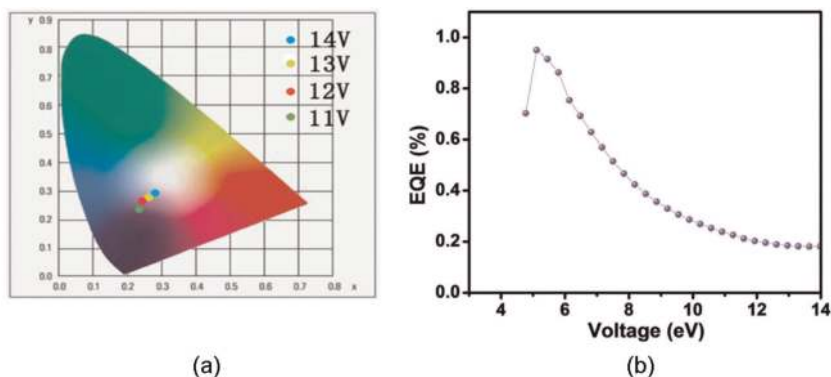


Figure 12.

(a) CIE coordinate at varied applied voltage of where CIE closer to that of pure white light (0.33, 0.33) at 14 V, (b) The EQE of this WLED was 0.24%, 0.21%, 0.20%, and 0.19% for 11, 12, 13, and 14 V applied voltages respectively.

4. Conclusion

CQDs have remarkable potential for PV use due to their large surface area, high conductivity, and rapid charge transfer. CQDs have been employed in a variety of solar cells as sensitizers and co-sensitizers, energy downshifting layers (EDSL), ETL, and hole transport materials (HTM), and their inclusion has enhanced the overall efficiency of solar cells. In addition, solar panels perform better when CQDs are included in the encapsulation layer.

Although warm WLEDs with a high color quality can now be realised using R-CQDs with long-wavelength and highly efficient emission, doing so is still challenging. Hardly reported SCWE-CQDs due to their surface defect-state emission character usually displayed faint emissions. Because of this, bandgap SCWE-CQDs with high QYs and solubility are urgently needed to enhance the luminescence and carrier transfer performance of SCWE-CQD-based electroluminescent WLEDs. Furthermore, highly effective electroluminescent WLEDs require efficient CQDs with triplet-excited-state involved features, such as room-temperature phosphorescence and thermally induced delayed fluorescence.

Author details

Pawan Kumar¹, Shweta Dua², Balaram Pani³ and Geeta Bhatt^{4*}

1 Department of Electronic Science, University of Delhi, India


2 Bhaskaracharya College of Applied Sciences, University of Delhi, India

3 University of Delhi, India

4 Non-Collegiate Women Education Board, University of Delhi, India

*Address all correspondence to: geeta.bhatt@bcas.du.ac.in

IntechOpen

© 2022 The Author(s). Licensee IntechOpen. This chapter is distributed under the terms of the Creative Commons Attribution License (<http://creativecommons.org/licenses/by/3.0>), which permits unrestricted use, distribution, and reproduction in any medium, provided the original work is properly cited. 

References

- [1] Kumar P, Dua S, Kaur R, Kumar M, Bhatt G. A review on advancements in carbon quantum dots and their application in photovoltaics. *RSC Advances*. 2022;**12**(8):4714-4759. DOI: 10.1039/D1RA08452F
- [2] Xu X, Ray R, Gu Y, Ploehn HJ, Gearheart L, Raker K, et al. Electrophoretic analysis and purification of fluorescent single-walled carbon nanotube fragments. *Journal of the American Chemical Society*. 2004; **126**(40):12736-12737. DOI: 10.1021/ja040082h
- [3] Wang Y, Hu A. Carbon quantum dots: synthesis, properties and applications. *Journal of Materials Chemistry C*. 2014; **2**(34):6921-6939. DOI: 10.1039/C4TC00988F
- [4] Kumar P, Bhatt G, Kaur R, Dua S, Kapoor A. Synthesis and modulation of the optical properties of carbon quantum dots using microwave radiation. *Fullerenes, Nanotubes and Carbon Nanostructures*. 2020;**28**(9):724-731. DOI: 10.1080/1536383X.2020.1752679
- [5] Izatt RM, Izatt SR, Bruening RL, Izatt NE, Moyer BA. Challenges to achievement of metal sustainability in our high-tech society. *Chemical Society Reviews*. 2014;**43**(8):2451-2475. DOI: 10.1039/C3CS60440C
- [6] Mirtchev P, Henderson EJ, Soheilnia N, Yip CM, Ozin GA. Solution phase synthesis of carbon quantum dots as sensitizers for nanocrystalline TiO₂ solar cells. *Journal of Materials Chemistry*. 2012;**22**(4):1265-1269. DOI: 10.1039/C1JM14112K
- [7] Baker SN, Baker GA. Luminescent carbon nanodots: emergent nanolights. *Angewandte Chemie International Edition*. 2010;**49**(38):6726-6744. DOI: 10.1002/anie.200906623
- [8] He P, Shi Y, Meng T, Yuan T, Li Y, Li X, et al. Recent advances in white light-emitting diodes of carbon quantum dots. *Nanoscale*. 2020;**12**(8):4826-4832. DOI: 10.1039/C9NR10958G
- [9] Yuan F, Li S, Fan Z, Meng X, Fan L, Yang S. Shining carbon dots: synthesis and biomedical and optoelectronic applications. *Nano Today*. 2016;**11**(5): 565-586. DOI: 10.1016/j.nantod.2016.08.006
- [10] Meng T, Yuan T, Li X, Li Y, Fan L, Yang S. Ultrabroad-band, red sufficient, solid white emission from carbon quantum dot aggregation for single component warm white light emitting diodes with a 91 high color rendering index. *Chemical Communications*. 2019; **55**(46):6531-6534. DOI: 10.1039/C9CC01794A
- [11] Yuan T, Yuan F, Li X, Li Y, Fan L, Yang S. Fluorescence-phosphorescence dual emissive carbon nitride quantum dots show 25% white emission efficiency enabling single-component WLEDs. *Chemical Science*. 2019;**10**(42): 9801-9806. DOI: 10.1039/C9SC03492G
- [12] Sharma K, Sharma V, Sharma SS. Dye-sensitized solar cells: fundamentals and current status. *Nanoscale Research Letters*. 2018;**13**(1):1-46. DOI: 10.1186/s11671-018-2760-6
- [13] Molaei MJ. The optical properties and solar energy conversion applications of carbon quantum dots: a review. *Solar Energy*. 2020;**196**:549-566. DOI: 10.1016/j.solener.2019.12.036
- [14] Han X, Zhong S, Pan W, Shen W. A simple strategy for synthesizing highly

luminescent carbon nanodots and application as effective down-shifting layers. *Nanotechnology*. 2015;**26**(6): 065402. DOI: 10.1088/0957-4484/26/6/065402

[15] Riaz R, Ali M, Maiyalagan T, Anjum AS, Lee S, Ko MJ, et al. Dye-sensitized solar cell (DSSC) coated with energy down shift layer of nitrogen-doped carbon quantum dots (N-CQDs) for enhanced current density and stability. *Applied Surface Science*. 2019; **483**:425-431. DOI: 10.1016/j.apsusc.2019.03.236

[16] Ali M, Riaz R, Bae S, Lee HS, Jeong SH, Ko MJ. Layer-by-Layer self-assembly of hollow nitrogen-doped carbon quantum dots on cationized textured crystalline silicon solar cells for an efficient energy down-shift. *ACS Applied Materials & Interfaces*. 2020; **12**(9):10369-10381. DOI: 10.1021/acscami.9b21087

[17] Lv T, Tang Y, Fan H, Liu S, Zeng S, Liu W. Carbon quantum dots anchored on the anti-reflection silica layer as solid luminescence down-shifting materials in solar panel encapsulation. *Solar Energy Materials and Solar Cells*. 2022;**235**: 111450. DOI: 10.1016/j.solmat.2021.111450

[18] Essner JB, Baker GA. The emerging roles of carbon dots in solar photovoltaics: a critical review. *Environmental Science: Nano*. 2017; **4**(6):1216-1263. DOI: 10.1039/C7EN00179G

[19] Gao N, Huang L, Li T, Song J, Hu H, Liu Y, et al. Application of carbon dots in dye-sensitized solar cells: a review. *Journal of Applied Polymer Science*. 2020;**137**(10): 48443. DOI: 10.1002/app.48443

[20] Wang H, Sun P, Cong S, Wu J, Gao L, Wang Y, et al. Nitrogen-doped

carbon dots for “green” quantum dot solar cells. *Nanoscale Research Letters*. 2016;**11**(1):1-6. DOI: 10.1186/s11671-016-1231-1

[21] Mistry B, Machhi HK, Vithalani RS, Patel DS, Modi CK, Prajapati M, et al. Harnessing the N-dopant ratio in carbon quantum dots for enhancing the power conversion efficiency of solar cells. *Sustainable Energy & Fuels*. 2019;**3**(11): 3182-3190. DOI: 10.1039/C9SE00338J

[22] Yang Q, Yang W, Zhang Y, Ge W, Yang X, Yang P. Precise surface state control of carbon quantum dots to enhance charge extraction for solar cells. *Nanomaterials*. 2020;**10**(3):460. DOI: 10.3390/nano10030460

[23] Singh T, Singh J, Miyasaka T. Role of metal oxide electron-transport layer modification on the stability of high performing perovskite solar cells. *ChemSusChem*. 2016;**9**(18):2559-2566. DOI: 10.1002/cssc.201601004

[24] Yan L, Yang Y, Ma CQ, Liu X, Wang H, Xu B. Synthesis of carbon quantum dots by chemical vapor deposition approach for use in polymer solar cell as the electrode buffer layer. *Carbon*. 2016;**109**:598-607. DOI: 10.1016/j.carbon.2016.08.058

[25] Li H, Shi W, Huang W, Yao EP, Han J, Chen Z, et al. Carbon quantum dots/TiO_x electron transport layer boosts efficiency of planar heterojunction perovskite solar cells to 19%. *Nano Letters*. 2017;**17**(4):2328-2335. DOI: 10.1021/acs.nanolett.6b05177

[26] Zhu X, Sun J, Yuan S, Li N, Qiu Z, Jia J, et al. Efficient and stable planar perovskite solar cells with carbon quantum dots-doped PCBM electron transport layer. *New Journal of Chemistry*. 2019;**43**(18):7130-7135. DOI: 10.1039/C8NJ06146G

- [27] Park S, Lee H, Park SW, Kim TE, Park SH, Jung YK, et al. Improved exciton dissociation efficiency by a carbon-quantum-dot doped work function modifying layer in polymer solar cells. *Current Applied Physics*. 2021;**21**:140-146. DOI: 10.1016/j.cap.2020.10.019
- [28] Pitchaiya S, Natarajan M, Santhanam A, Asokan V, Yuvapragasam A, Ramakrishnan VM, et al. A review on the classification of organic/inorganic/carbonaceous hole transporting materials for perovskite solar cell application. *Arabian Journal of Chemistry*. 2020;**13**(1): 2526-2557. DOI: 10.1016/j.arabjc.2018.06.006
- [29] Vercelli B. The role of carbon quantum dots in organic photovoltaics: a short overview. *Coatings*. 2021;**11**(2): 232. DOI: 10.3390/coatings11020232
- [30] Paulo S, Stoica G, Cambarau W, Martinez-Ferrero E, Palomares E. Carbon quantum dots as new hole transport material for perovskite solar cells. *Synthetic Metals*. 2016;**222**:17-22. DOI: 10.1016/j.synthmet.2016.04.025
- [31] Nguyen DN, Roh SH, Kim DH, Lee JY, Wang DH, Kim JK. Molecular manipulation of PEDOT: PSS for efficient hole transport by incorporation of N-doped carbon quantum dots. *Dyes and Pigments*. 2021;**194**:109610. DOI: 10.1016/j.dyepig.2021.109610
- [32] Feng X, Zhao Y, Yan L, Zhang Y, He Y, Yang Y, et al. Low-temperature hydrothermal synthesis of green luminescent carbon quantum dots (CQD), and optical properties of blends of the CQD with poly (3-hexylthiophene). *Journal of Electronic Materials*. 2015;**44**(10): 3436-3443. DOI: 10.1007/s11664-015-3893-3
- [33] Cui B, Yan L, Gu H, Yang Y, Liu X, Ma CQ, et al. Fluorescent carbon quantum dots synthesized by chemical vapor deposition: an alternative candidate for electron acceptor in polymer solar cells. *Optical Materials*. 2018;**75**:166-173. DOI: 10.1016/j.optmat.2017.10.010
- [34] Privitera A, Righetto M, Mosconi D, Lorandi F, Isse AA, Moretto A, et al. Boosting carbon quantum dots/fullerene electron transfer via surface group engineering. *Physical Chemistry Chemical Physics*. 2016;**18**(45): 31286-31295. DOI: 10.1039/C6CP05981C
- [35] Shejale KP, Jaiswal A, Kumar A, Saxena S, Shukla S. Nitrogen doped carbon quantum dots as Co-active materials for highly efficient dye sensitized solar cells. *Carbon*. 2021;**183**: 169-175. DOI: 10.1016/j.carbon.2021.06.090
- [36] Sivagami D, Priyadarshini BG. Role of carbon quantum dot for enhanced performance of photo-absorption in Cu₂CoSnS₄ superstrate solar cell device. *Materials Advances*. 2022;**3**(5):2405-2416. DOI: 10.1039/D1MA01117K
- [37] Kumari R, Sahu SK. A new insights into multicolor emissive carbon dots using *Trachelospermum jasminoides* leaves for the application of WLEDs. *Colloids and Surfaces A: Physicochemical and Engineering Aspects*. 2022;**647**:128959. DOI: 10.1016/j.colsurfa.2022.128959
- [38] Cui B, Feng XT, Zhang F, Wang YL, Liu XG, Yang YZ, et al. The use of carbon quantum dots as fluorescent materials in white LEDs. *New Carbon Materials*. 2017;**32**(5):385-401. DOI: 10.1016/S1872-5805(17)60130-6

- [39] Zheng J, Wang Y, Zhang F, Yang Y, Liu X, Guo K, et al. Microwave-assisted hydrothermal synthesis of solid-state carbon dots with intensive emission for white light-emitting devices. *Journal of Materials Chemistry C*. 2017;5(32):8105-8111. DOI: 10.1039/C7TC01701D
- [40] Wang Z, Yuan F, Li X, Li Y, Zhong H, Fan L, et al. 53% efficient red emissive carbon quantum dots for high color rendering and stable warm white-light-emitting diodes. *Advanced Materials*. 2017;29(37):1702910. DOI: 10.1002/adma.201702910
- [41] Zhu J, Bai X, Chen X, Shao H, Zhai Y, Pan G, et al. Spectrally tunable solid state fluorescence and room-temperature phosphorescence of carbon dots synthesized via seeded growth method. *Advanced Optical Materials*. 2019;7(9):1801599. DOI: 10.1002/adom.201801599
- [42] Li W, Wu M, Jiang H, Yang L, Liu C, Gong X. Carbon dots/ZnO quantum dots composite-based white phosphors for white light-emitting diodes. *Chemical Communications*. 2011;58(12):1910-1913. DOI: 10.1039/D1CC06180A
- [43] Yuan, F., Wang, Z., Li, X., Li, Y., Tan, Z.A., Fan, L. and Yang, S. Bright multicolor bandgap fluorescent carbon quantum dots for electroluminescent light-emitting diodes. *Advanced Materials*, 2017, 29(3), p. 1604436. DOI: 10.1002/adma.201604436
- [44] Jia H, Wang Z, Yuan T, Yuan F, Li X, Li Y, et al. Electroluminescent warm white light-emitting diodes based on passivation enabled bright red bandgap emission carbon quantum dots. *Advanced Science*. 2019;6(13):1900397. DOI: 10.1002/advs.201900397
- [45] Paulo-Mirasol S, Martínez-Ferrero E, Palomares E. Direct white light emission from carbon nanodots (C-dots) in solution processed light emitting diodes. *Nanoscale*. 2019;11(23):11315-11321. DOI: 10.1039/C9NR02268F
- [46] Luo Z, Qi G, Chen K, Zou M, Yuwen L, Zhang X, et al. Microwave-assisted preparation of white fluorescent graphene quantum dots as a novel phosphor for enhanced white-light-emitting diodes. *Advanced Functional Materials*. 2016;26(16):2739-2744. DOI: 10.1002/adfm.201505044
- [47] Rao L, Zhang Q, Wen M, Mao Z, Wei H, Chang HJ, et al. Solvent regulation synthesis of single-component white emission carbon quantum dots for white light-emitting diodes. *Nanotechnology Reviews*. 2021; 10(1):465-477. DOI: 10.1515/ntrev-2021-0036